Electronic Supporting information for

Microstring-engineered tension tissues: A novel platform for replicating tissue mechanics and advancing mechanobiology

Zixing Zhou[a], Tingting Li[a], Wei Cai[a], Xiaobin Zhu[b], Zuoqi Zhang[a], Guoyou Huang[*a]

[a] Department of Engineering Mechanics, School of Civil Engineering, Wuhan University, Wuhan 430072, P.R. China

[b] Department of Spine Surgery and Musculoskeletal Tumor, Zhongnan Hospital of Wuhan University, Wuhan 430072, P.R. China

*Corresponding author: Guoyou Huang, Email: gyhuang@whu.edu.cn

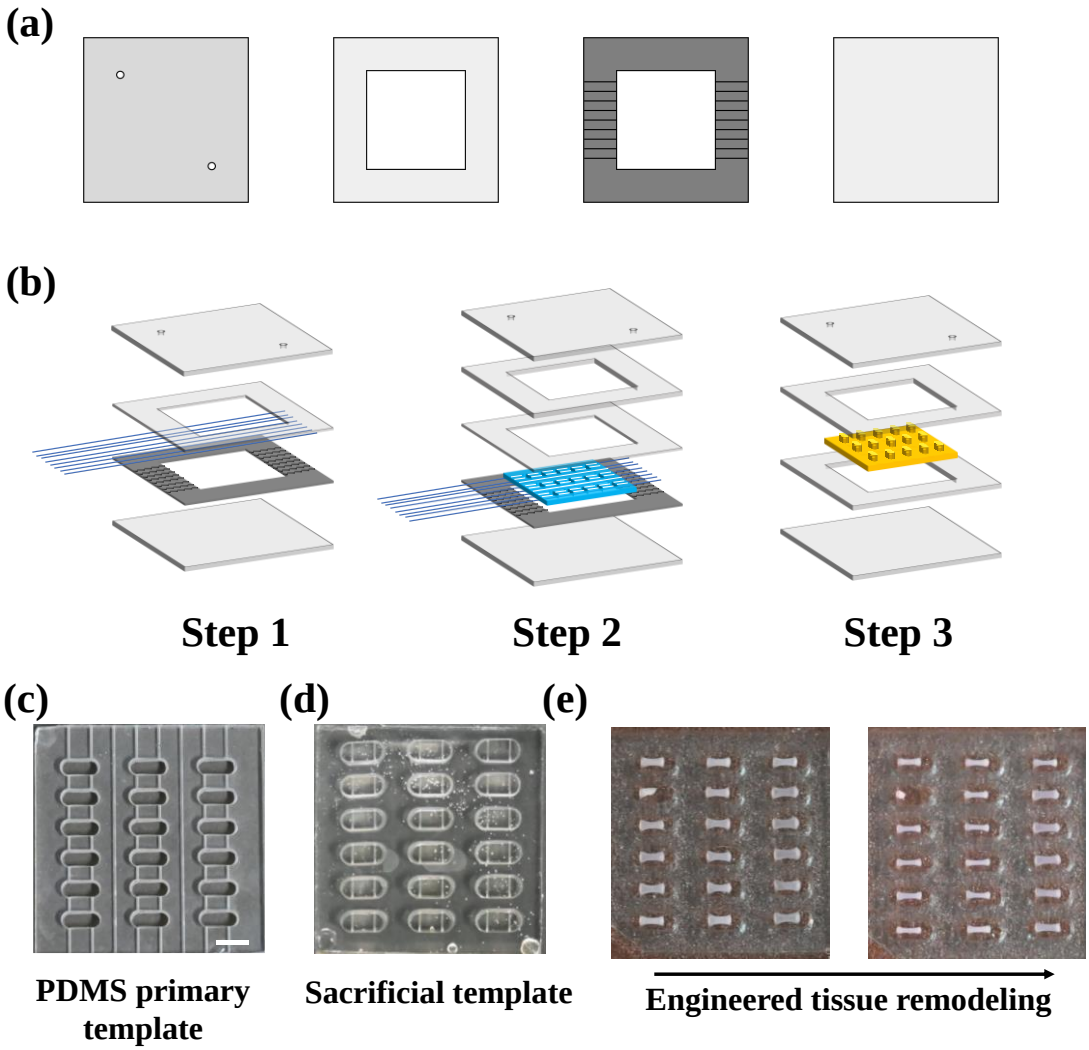

Fig. S1. Fabrication of the microstring chips for engineering tension tissues. (a) Schematic illustration of the mold components: top cover, intermediate layering cover, custom stainless steel cover, and bottom cover. (b) Schematic illustration of the mold assembly sequence, showing the three major steps. (c) Photograph of the initial PDMS template. (d) Photograph of the gelatin sacrificial template. (e) Photograph of the cultured microstring-engineered tension tissues (METTs). Scale bar: 3 mm.

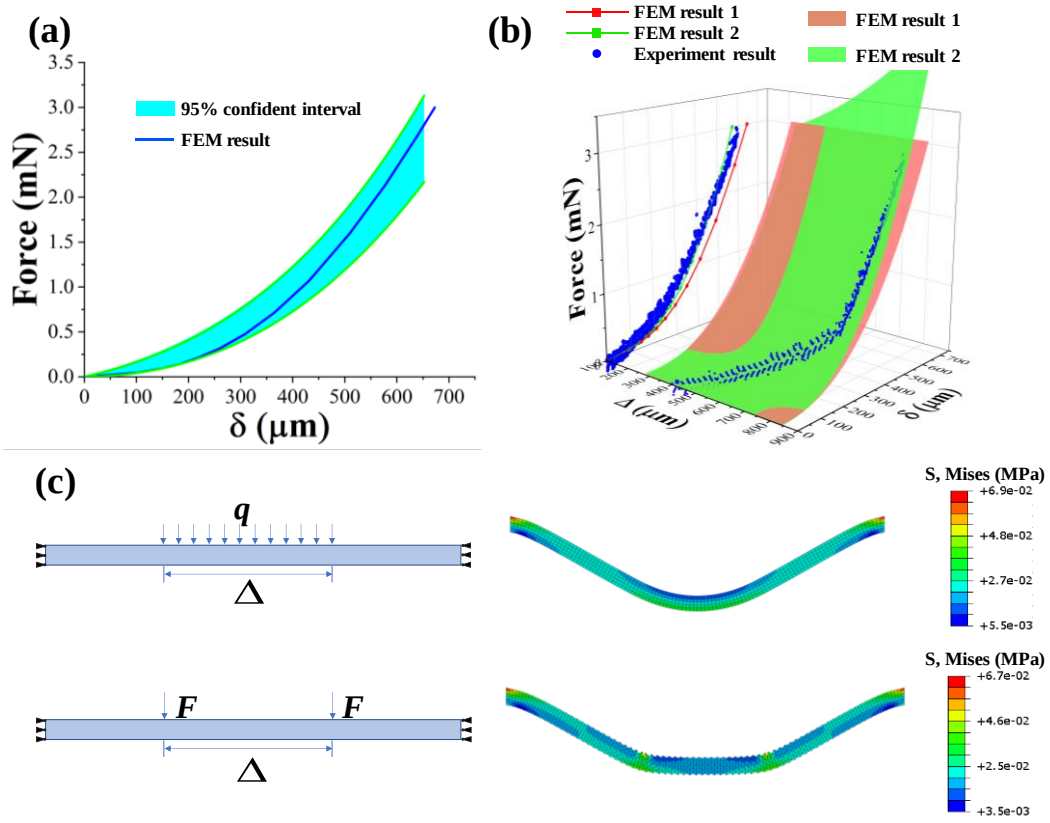

Fig. S2. Calibration of microstrings via bending tests and finite element analysis. (a) Results of the concentrated load bending test and corresponding finite element calculations, used for calibrating the Young's modulus of the microstrings. (b) Results of the bending test using a custom-designed coarse probe, compared with the upper and lower limit surfaces obtained from finite element calculations. (c) Finite element simulation of microstring deformation under the contraction force of tissues with a certain width, simulating two extreme cases.

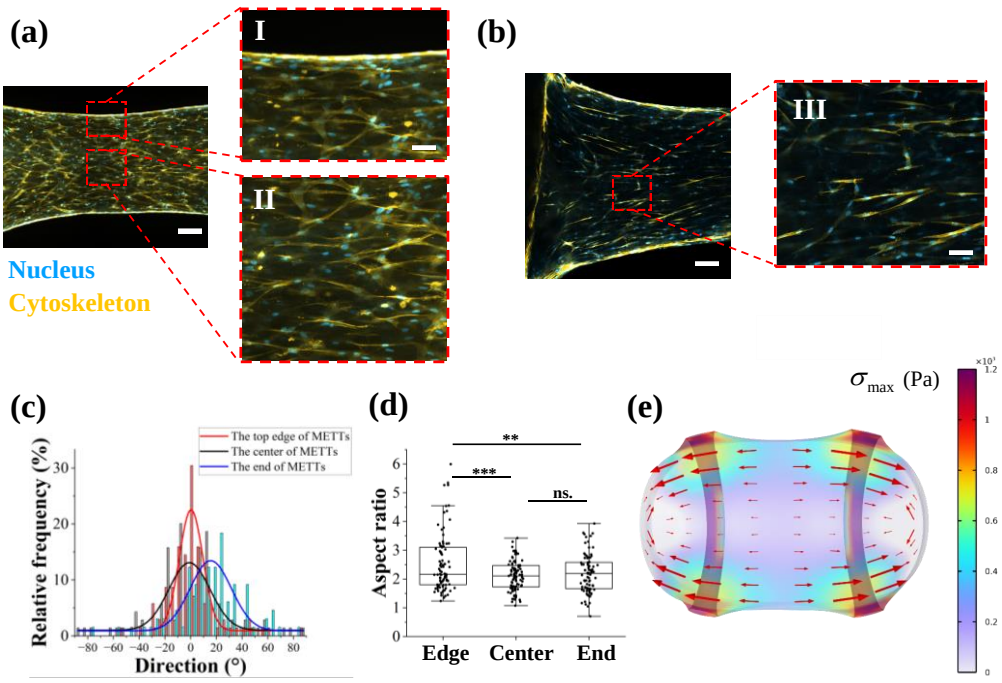

Fig. S3. Characterization of cellular morphology in different locations of METTs and simulation model of tissue contraction**.** (a) Fluorescence images of cell nuclei and cytoskeleton at the top edge and center of METTs, with scale bars 100 μm (left) and 300 μm (right). (b) Fluorescence images of cell nuclei and cytoskeleton near the ends of METTs, with scale bars 100 μm (left) and 300 μm (right). (c) Comparison of cell orientation across the three distinct locations in METTs. (d) Comparison of the cell length-to-width ratio at these locations. Statistical significance was assessed using an unpaired t-test, with $^{**}p < 0.01$, $^{***}p < 0.001$ indicating significance. (e) Simulation results of the METT contraction process, where red arrows indicate the direction of the principal stress, with arrow lengths representing the magnitude of the stress.

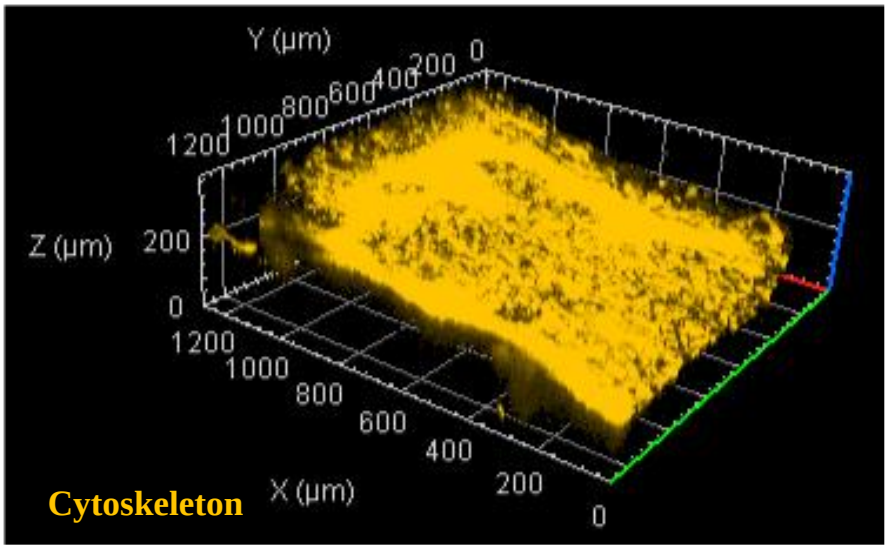

Fig. S4. Three-dimensional reconstruction of a METT based on confocal microscopy.

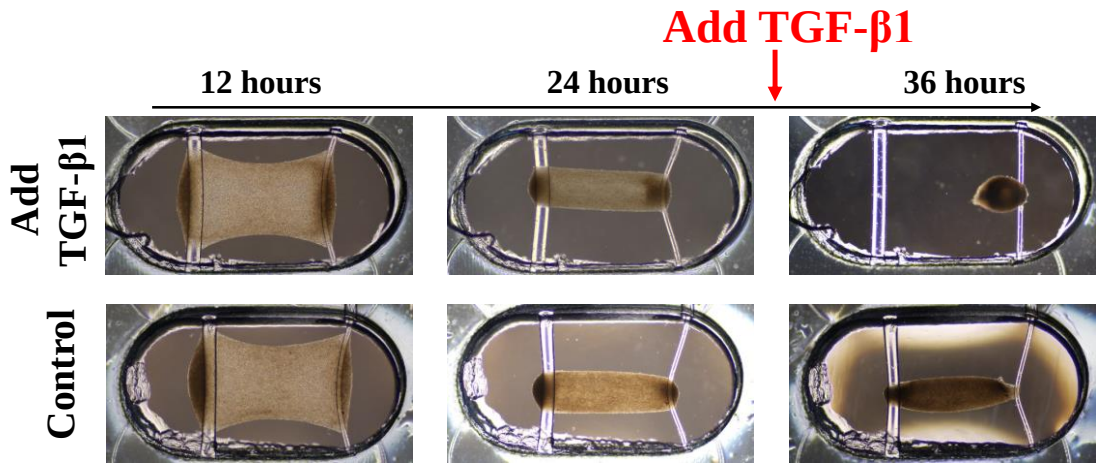

Fig. S5. Photographs of the in vitro tissue culture process of METTs with BMMSCs at a cell concentration of 5×10^6 cells/mL.